Impact of thermomechanical pretreatment by twin-screw extrusion on the properties of bio-based materials from sugarcane bagasse obtained by thermocompression

Julie Cavailles, Guadalupe Vaca-Medina, Jenny Wu-Tiu-Yen, Laurent Labonne, Philippe Evon, Jérôme Peydecastaing, Pierre-Yves Pontalier

Bioresource Technology 414 (2024) 131642

Contents lists available at ScienceDirect

Bioresource Technology

journal homepage: www.elsevier.com/locate/biortech

Impact of thermomechanical pretreatment by twin-screw extrusion on the properties of bio-based materials from sugarcane bagasse obtained by thermocompression

Julie Cavailles [a,b,*], Guadalupe Vaca-Medina [a], Jenny Wu-Tiu-Yen [b], Laurent Labonne [a], Philippe Evon [a], Jérôme Peydecastaing [a], Pierre-Yves Pontalier [a]

[a] Laboratoire de Chimie Agro-industrielle (LCA), Université de Toulouse, INRAE, Toulouse INP, 4 Allée Emile Monso, 31030 Toulouse Cedex 4, France
[b] eRcane, La Réunion, Sainte-Clotilde, France

HIGHLIGHTS

- Bio-based materials were produced by thermocompression from SCB extrudates.
- Twin-screw extrusion facilitated fiber defibration and particle size reduction.
- Materials from extrudate showed superior mechanical properties and water resistance.
- High flexural properties achieved with 1.25 L/S ratio and restrictive screw profile.
- Best water resistance observed with 0.4 L/S ratio and more shearing screw profile.

GRAPHICAL ABSTRACT

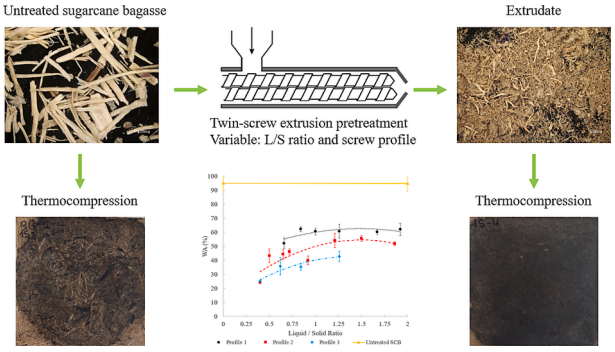

ARTICLE INFO

Keywords:
Twin-screw extrusion
Sugarcane bagasse
Bio-based materials
Thermocompression
Screw profile

ABSTRACT

The aim of this study was to produce binderless materials by thermocompression from lignocellulosic biomass pretreated using twin-screw extrusion. The impact of twin-screw extrusion pretreatment on sugarcane bagasse (SCB) was evaluated, along with the effects of two associated parameters: the liquid-to-solid (L/S) ratio and the screw profile, using three different mechanical shear rates. It was shown that twin-screw extrusion pretreatment resulted in materials with improved properties as compared to those obtained with untreated SCB. The mechanical properties and water resistance of materials obtained after pretreatment were mainly impacted by the screw profile. The flexural modulus increased from 5.3 to 6.1 GPa and the flexural strength from 39.0 to 55.5 MPa. Water absorption (WA) from the thermocompressed materials ranged from 25 to 62 %, and thickness swelling (TS) from 24 to 67 %. Materials obtained with a 0.4 L/S ratio had lower flexural strength but the best water resistance. For the same L/S ratio, the use of a more shearing screw profile improved the material properties, especially the water resistance. The best material was produced with pretreated SCB using a 1.25 L/S

* Corresponding author at: 4 Allée Emile Monso, 31030 Toulouse, France.
E-mail addresses: julie.cavailles@toulouse-inp.fr (J. Cavailles), guadalupe.vacamedina@toulouse-inp.fr (G. Vaca-Medina), jenny.wutiuyen@ercane.re (J. Wu-Tiu-Yen), laurent.labonne@toulouse-inp.fr (L. Labonne), philippe.evon@toulouse-inp.fr (P. Evon), jerome.peydecastaing@toulouse-inp.fr (J. Peydecastaing), pierreyves.pontalier@toulouse-inp.fr (P.-Y. Pontalier).

https://doi.org/10.1016/j.biortech.2024.131642
Received 5 August 2024; Received in revised form 7 October 2024; Accepted 13 October 2024
Available online 15 October 2024

ratio with the most restrictive screw profile, resulting in materials with a 5.6 GPa flexural modulus, 55.5 MPa flexural strength, and WA and TS values of 44 % and 42 %, respectively.

1. Introduction

Sugarcane (*Saccharum officinarum*), a major agricultural crop of the Gramineae family, is extensively cultivated in tropical and subtropical regions. The estimated global production in 2021 was 1.9 billion t (FAO, 2021). Sugar production from sugarcane generates substantial by-products, including cane trash, bagasse, molasses and press mud (Singh et al., 2021). Sugarcane bagasse (SCB)—the fibrous residue remaining after juice extraction—is the primary by-product of the sugar cane industry, with 1 t of sugarcane producing 0.3 t of bagasse (wet basis). The resulting high abundance of SCB, which has a net calorific value of 9.7 MJ/kg, is predominantly used as feedstock for energy production (Arshad and Ahmed, 2016). SCB is mainly composed of lignocellulosic components and as such it is a vital resource for energy production or manufacturing bio-based products in a sustainable development framework (Anwar et al., 2014; Meghana and Shastri, 2020). In lignocellulosic matter, cellulose is embedded in a cross-linked matrix of hemicelluloses surrounded by lignin, which hampers access to the sugar content. The development of efficient processes to transform this biomass is essential for new emerging applications. Given the complexity and variability of the biomass chemistry and structure, innovative approaches are necessary to process biomass into high value compounds. Research findings have shown that SCB can be used to produce biofuels, animal feed, industrial enzymes, sugars and oligosaccharides, biosorbents and commercial chemicals, while also serving as feedstock for gasification (Alokika et al., 2021).

SCB also has high potential as a bio-based raw material for manufacturing fiberboards and food packaging. However, bagasse-based material production typically involves pulping, which requires several chemical treatments, including the addition of chemical agents such as resins, plasticizers or water and oil repellents (Semple et al., 2022; Sugahara et al., 2019). Thermocompression is a molding process that enables the production of cohesive lignocellulosic materials without the need for pulping, binders or chemical agents. This method has been successfully applied to SCB for the production of cohesive binderless (i.e. no exogenous binder added) fiberboards (Cavailles et al., 2024a, 2024b; Nadhari et al., 2020; Nonaka et al., 2013; Widyorini et al., 2005).

However, these latter studies did not focus on the effects of pretreating SCB before its transformation into materials. Adding a pretreatment could break down the SCB lignocellulosic structure, thereby making the target elements more accessible for internal reorganization upon thermocompression, while potentially enhancing the properties of the resulting materials. Various types of lignocellulosic biomass pretreatments exist, which are physical, biological, chemical and physicochemical in nature (Alokika et al., 2021; Harmsen et al., 2010; Karp et al., 2013; Mankar et al., 2021). Physical pretreatments include milling, extrusion, irradiation, microwave and ultrasound. Chemical pretreatments range from acid hydrolysis, alkaline hydrolysis, organosolv treatment, oxidative delignification, and extraction using ionic liquids, supercritical fluids or deep eutectic solvents. Biological pretreatments involve microorganisms such as fungi or bacteria. Finally, physicochemical pretreatments include steam explosion, ammonia fiber explosion (AFEX), CO_2 explosion, liquid hot water treatment and wet oxidation. Otherwise, twin-screw extrusion is a very promising thermomechanical process for SCB pretreatment.

Twin-screw extrusion offers numerous possibilities for biomass fractionation and processing (Evon et al., 2018), such as mechanical pressing and extraction of vegetable oil (Evon et al., 2013, 2009; Sriti et al., 2012; Uitterhaegen et al., 2015; Uitterhaegen and Evon, 2017), hemicellulose extraction (N'Diaye and Rigal, 2000; Zeitoun, 2010; Zheng, 2016), enzymatic degradation of plant cell walls for second-generation bioethanol (Chen et al., 2011; Duque et al., 2018; Kang et al., 2013; Lamsal et al., 2010; Vandenbossche et al., 2016) or biogas (Pérez-Rodríguez et al., 2017) production, biocomposite material production (Alvarez et al., 2005; Anuar et al., 2012; Gamon et al., 2013; Sasimowski et al., 2021; Uitterhaegen et al., 2018), and defibration of lignocellulosic materials (Gao et al., 2019; Rouilly et al., 2006; Theng et al., 2019). Twin-screw extrusion functions as a thermo-mechano-chemical reactor capable of continuously transforming and/or fractionating biomass. The thermal, mechanical and/or chemical operations are controlled by selecting appropriate screw elements along the screw profile, adjusting the screw speed, regulating the barrel temperature, and injecting liquid reagents or additives along the barrel (Konan et al., 2022; Zheng and Rehmann, 2014).

Thermomechanical pretreatment by twin-screw extrusion is particularly interesting for producing binderless materials via thermocompression as it breaks down the lignocellulosic structure of the biomass (Theng et al., 2019). The inner cell wall components become more accessible, and the properties of the obtained materials are modified. This process increases fiber accessibility and promotes self-adhesion during material manufacturing, thereby improving the fiber morphology and boosting the fiber aspect ratio. Twin-screw extrusion has been proposed as a promising solution for the defibration of various biomass sources, such as rice (Theng et al., 2019) and coriander (Uitterhaegen et al., 2017) straws, sunflower cake from whole plants (Evon et al., 2014), and oleaginous flax shives (Evon et al., 2021). The extrudates obtained in these studies were mixtures of lignocellulosic fibers that could be transformed by thermocompression into bio-based materials. SCB extrusion has primarily been studied for biorefinery applications to enhance yields of glucose and xylose released after enzymatic hydrolysis (da Silva et al., 2013; Kuster Moro et al., 2017; Vandenbossche et al., 2016), and for preparing biocomposites with a polymer matrix (Ramaraj, 2007; Wang et al., 2013). The use of twin-screw extrusion as an SCB pretreatment process prior to binderless thermocompression for material production is a novel approach that has recently begun to be explored (Cavailles et al., 2024a). The latter involved comparing two twin-screw extrusion configurations with and without filtration. The results revealed enhancement in the material properties when the process was supplemented by twin-screw extrusion pretreatment, with or without filtration—this included a 2-fold increase in the mechanical properties, as well as a 2-fold reduction in water absorption (WA) and thickness swelling (TS). Moreover, in the configuration with filtration, the study highlighted the role of water in facilitating transport of the mixture, improving the solubilization of the molecules through better bagasse impregnation and pressing of the mixture. However, the impact of the twin-screw extrusion conditions on the configuration without filtration was not assessed, thus calling for further research to understand how the pretreatment modifies SCB and influences the material properties.

In this context, the aim of the present study was to investigate thermomechanical pretreatment of SCB by twin-screw extrusion to modify its structure and to gain insight into the effects of pretreatment on the extrudate characteristics and the material properties obtained after thermocompression without the addition of exogenous binder. The impact of twin-screw extrusion pretreatment on the SCB characteristics, and on the properties of the resulting bio-based materials was assessed in comparison to untreated SCB, as a reference. Various processing conditions, with several degrees of severity, were tested by varying the liquid-to-solid (L/S) ratio used for extrudate production as well as the screw profile configurations, with three increasing shear levels.

2. Materials and methods

2.1. Raw material preparation

Air-dried SCB was provided by eRcane (Réunion, France). Raw SCB was ground using an Electra F6 N V knife mill (Paris, France) with a 16-mm grid to homogenize the particle size before pretreatment. SCB was then moistened by spraying water to achieve 30 % (w/w) water content, thus promoting fine particle aggregation with long fibers. This step aimed to reduce particle and fiber segregation in the solid feeder hopper during the twin-screw extrusion trials, while ensuring a stable homogeneous SCB feed rate. Moreover, a portion of the raw SCB was ground using a 2-mm grid on an IKA Werke MF 10 basic microfine grinder drive (Staufen im Breisgau, Germany) for chemical composition characterization.

2.2. Twin-screw extrusion pretreatment

SCB was subjected to thermomechanical treatment using a co-penetrating and co-rotating Clextral BC45 twin-screw extruder (Firminy, France) to produce extrudates for material manufacture. The extruder consisted of seven modules along the barrel, each 20 cm long. Modules 2 to 7 were heated by thermal induction and cooled by water circulation. SCB was fed into the extruder in the first module using a solid feeder, and water was injected at the end of module 2 using a Clextral DKM K20-2-PP16 piston pump (Firminy, France). Three different screw profiles were used during this study (Fig. 1). After liquid injection, a series of 2-lobe kneading blocks (BB 10x10 90°), each 100 mm in length, were positioned at the end of module 4 to ensure intimate water-SCB mixing. Variations in the extruder shear zone were located in module 7. The reverse double-thread screw elements (CF2C) used in profile 1 were 50 mm long with a –33 mm pitch. In profile 2, they had the same length but a smaller pitch of −25 mm. In profile 3, the CF2C screws were longer (100 mm) with the same pitch as in profile 2. These three screw profiles allowed evaluation of the effects of pitch (profiles 1 and 2) and the length of the reverse screw elements (profiles 2 and 3), when different shear levels were applied, with profile 3 having the highest level.

The screw rotation speed (250 rpm), SCB feed rate (5 kg/h of dry matter), water inlet flow rates, and barrel temperature were monitored via a control panel. The preset temperatures for the modules along the barrel were 25, 25, 75, 100, 100, 100 and 100 °C for modules 1 to 7, respectively. The experimental variables in this study were the L/S ratio (ranging from 0.4 to 2 per profile under stable extrusion conditions) and the screw profile. The theoretical operating conditions are presented in Table 1.

The twin-screw extruder was operated for 5 min before each sampling to ensure stable operating conditions. Once the latter was reached, the extrudate was collected over a 10 min period to avoid any variability in the outlet flow rate. The sample collection time was measured with a stopwatch. For each tested condition, the extrudate was weighed and its water content was measured immediately after collection using a Sartorius MA35 infrared moisture balance (Göttingen, Germany). The extrudates were then stabilized by oven drying at 50 °C overnight and conditioned in a climatic chamber at 25 °C and 50 % relative humidity (RH) for 3 weeks until the moisture content had stabilized. This preparation was done before uniaxial thermocompression and physicochemical characterization of the extrudates.

2.3. Preparation of bio-based materials by uniaxial thermocompression

All SCB materials were produced by thermocompressing 20 g of untreated SCB or extrudates using a steel mold. A heated hydraulic press with a 50 t capacity (Pinette Emidecau Industries, Chalon-sur-Saône, France) was used to produce flat square materials measuring 70 mm × 70 mm. 102 MPa uniaxial pressure was applied, and the materials were then heated to 200 °C. The temperature was maintained for 10 min, and the mold was then cooled while maintaining pressure before opening

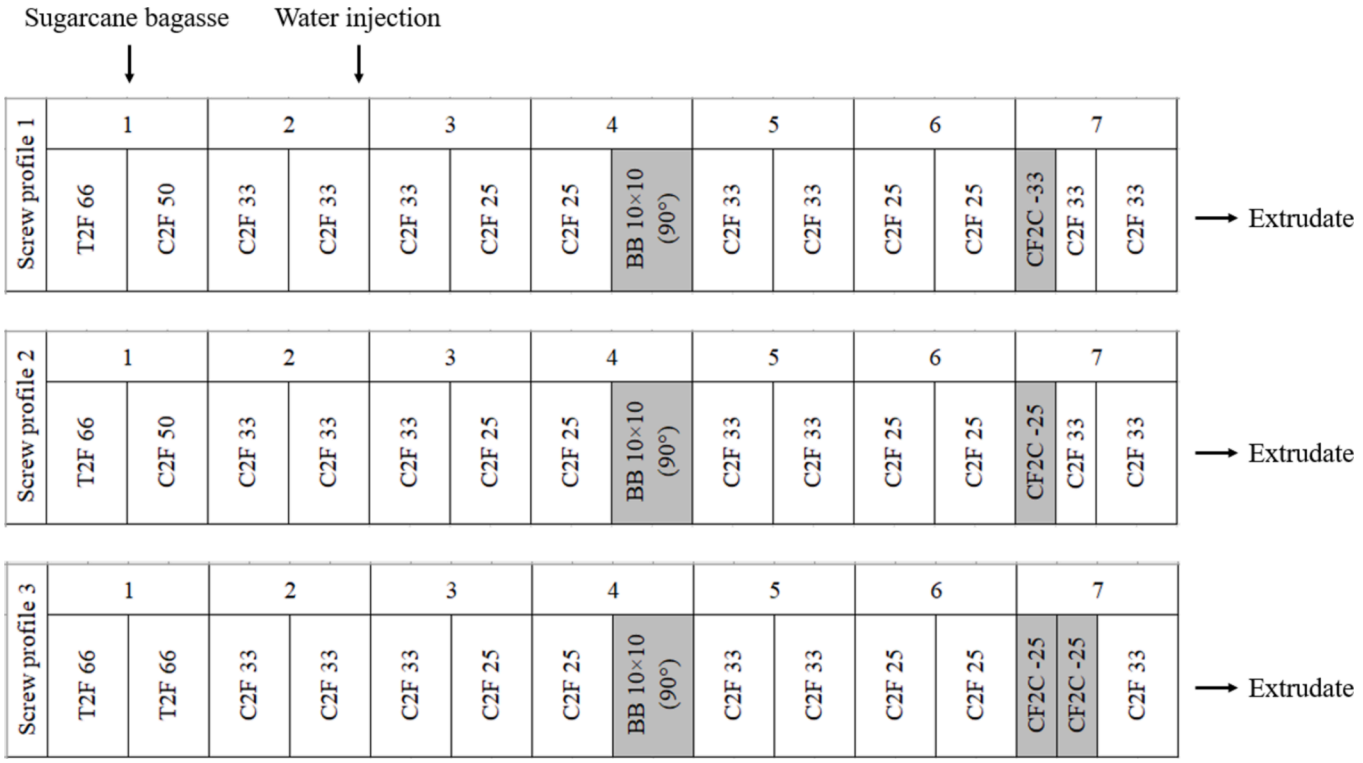

Fig. 1. Screw profile configurations for the SCB pretreatment using a Clextral BC45 twin-screw extruder. T2F: conveying trapezoidal double-flight screws; C2F: conveying conjugated double-flight screws; BB: 2-lobe kneading blocks; CF2C: reverse double-thread screw elements. The numbers following the type of screw element indicate the pitch of C2F, T2F and CF2C screws, and the length of the BB screws.

Table 1
Theoretical operating conditions used for extrudate production from SCB in a Clextral BC45 twin-screw extruder.

N°	Profile	L/S	MC_{SCB} (%)	Q_{SCB} (kg/h dry)	$Q_{water\ pump}$ (kg/h)	Q_L (kg/h)
1	1	0.70	30.2	5	1.3	3.5
2		0.85			2.1	4.3
3		1.00			2.8	5.0
4		1.25			4.1	6.3
5		1.50			5.3	7.5
6		2.00			7.8	10.0
7	2	0.40	29.5		0	2.0
8		0.55			0.7	2.8
9		0.70			1.4	3.5
10		0.85			2.2	4.3
11		1.00			2.9	5.0
12		1.25			4.2	6.3
13		1.50			5.4	7.5
14		2.00			7.8	10.0
15	3	0.40	29.7		0	2.0
16		0.70			1.4	3.5
17		1.00			2.9	5.0
18		1.25			7.9	10.0

Where QSCB and QL are the mass flow rates of SCB and total water, Qwater pump is the mass flow rate of water supplied by the pump, and MCSCB is the moisture content of the SCB input.

(Cavailles et al., 2024b). For each tested extrusion condition, two materials were produced and photographs were taken. The materials were cut into eight specimens, each 45 mm long and 10 mm wide, and stored in an environmental chamber at 25 °C and 50 % RH for 2 weeks until constant weight before property testing.

2.4. Chemical composition of raw SCB

The chemical composition of the raw SCB was determined in triplicate. The contents are expressed as a percentage of dry matter (DM). The DM content was evaluated by drying the sample at 105 °C until constant weight. The ash content was measured after mineralization at 550 °C for 12 h (Sluiter, 2008). Chemical characterization was carried out using an analytical procedure based on that developed by the National Renewable Energy Laboratory (NREL) (Sluiter et al., 2008). Briefly, water and ethanol extractable contents were determined after water and ethanol (96 %) extraction using 1 g of sample and 100 mL of boiled solvent for 1 h on a Foss Fibertech FT 122 extraction system (Hillerød, Denmark). The subsequent analyses were performed on the free-extractive material, and the results were reported relative to the raw biomass by accounting for the overall extractable content. Two-step hydrolysis was performed on the free-extractives material using 72 % sulfuric acid from VWR (Radnor, PA, USA) at 30 °C for 1 h, followed by a 4 % sulfuric acid solution with deionized water at 121 °C for 1 h, followed by filtration. The acid-insoluble lignin (AIL) content was measured gravimetrically after mineralization at 450 °C for 12 h. The acid-soluble lignin (ASL) content was determined in the liquid fraction using a Shimadzu UV-1800 spectrophotometer (Kyoto, Japan) at 240 nm with a 25 L/g.cm absorptivity constant. The liquid fraction was neutralized with $CaCO_3$ from Merck (Darmstadt, Germany) until reaching neutral pH and then filtered using a 0.2 μm cellulose acetate filter before HPLC analysis on a Thermo Ultimate 3000 HPLC system (Thermo Scientific, Sunnyvale, CA, USA). All HPLC standards (i.e. acetic acid, arabinose, glucose and xylose) were purchased from Sigma-Aldrich (Saint-Louis, MO, USA). A Rezex RHM-Monosaccharide H + column (300 × 7.8 mm) connected to a Rezex RHM-Monosaccharide H + guard column (50 × 7.8 mm), both from Phenomenex (Torrance, CA, USA), was used with 5 mmol/L H_2SO_4 as eluent at a 0.6 mL/min flow rate. The injection volume was 50 μL, with the column maintained at 65 °C and the RI detector at 50 °C.

2.5. SCB physical characterization

The particle size distributions of untreated SCB and extrudates were determined in triplicate using a Retsch AS 200 vibratory sieve shaker (Haan, Germany). 40 g samples were placed in the sieve shaker for 10 min at 1 mm amplitude using a series of six sieves with 6.3 mm, 4.0 mm, 2.0 mm, 1.0 mm, 0.8 mm and 0.2 mm mesh openings and a bottom plate. The material retained on each sieve was weighed and expressed as a percentage of the total weight. The fine particle fraction was defined as the fraction retained < 0.2 mm.

Optical images of the untreated SCB and extrudates were obtained using a Nikon SMZ1500 binocular microscope (Tokyo, Japan) equipped with a Nikon DMX 1200 camera (Tokyo, Japan). The optical images obtained were used to measure the length and diameter of the fibers and particles with an image processing tool to determine their aspect ratio (L/D) from around 100 measurements. A cumulative aspect ratio distribution was determined per sample.

SEM images of the untreated SCB and extrudates were obtained using a FEI Quanta 450 scanning electron microscope (Hillsboro, OR, USA), with 130 Pa water–vapor partial pressure in the chamber at high voltage (12.5 kV) and without sample coating.

Dynamic vapor sorption (DVS) analysis was performed on the untreated SCB and extrudates to determine their water adsorption and desorption isotherms and their water adsorption constants (c) using a DVS Advantage System (Surface Measurement System, Alperton, UK). Measurements were carried out throughout 18 different relative humidity (RH) steps (0–95 %), with a dm/dt of 2 × 10 − 3 %/min. The specific surface area (SSA) was determined by applying the Brunauer-Emmet-Teller (BET) theory (Brunauer et al., 1938) to the linear region of adsorption isotherms between 0.05 and 0.35 of P/P0.

The bulk and tapped densities of the untreated SCB and extrudates were determined using a Granuloshop Densitap ETD-20 volumenometer (Chatou, France) fitted with a 250 mL graduated cylinder. The sample was weighed in the graduated cylinder, and the volume was recorded before compaction to determine the bulk density. The cylinder was then tapped 500 times on the volumenometer at 3 mm height and a speed of 250 taps/min. The volume was measured to the nearest graduation and the process was repeated until a constant volume was obtained to determine the tapped density. All measurements were performed in triplicate.

2.6. Characterization of the thermocompressed materials

The density of the materials after thermocompression was determined using the pieces of material remaining after cutting the bending test specimens. The densities of these samples were assessed using a method based on Archimedes' principle, with cyclohexane as immersion liquid (Satyanarayana et al., 2018). Using a Sartorius hydrostatic balance (Göttingen, Germany) capable of weighing in both air and liquid media, we determined the density of our samples with the following formula according to the operating manual:

$$\text{Density} = \frac{w_{air}{}^{*}(d_{cyclohexane} - d_{air})}{(w_{air} - w_{cyclohexane})^{*}\text{Corr}} + d_{air} \quad (1)$$

where w_{air} and $w_{cyclohexane}$ are the sample weights measured in air and cyclohexane, d_{air} and $d_{cyclohexane}$ are the densities of air and cyclohexane at room temperature, and Corr is the thrust correction factor due to the submerged wire.

The compaction ratio of each material was calculated by dividing the density of the material by the bulk density of the raw material used (untreated SCB and extrudates).

The test specimen bending properties were assessed according to the ISO 16978:2003 standard (ISO 16978:2003 Wood-Based Panels – Determination of Modulus of Elasticity in Bending and of Bending Strength, 2003) using a Tinius Olsen universal testing machine

(Horsham, PA, USA) fitted with a 500 N load cell, and the three-point bending test. The sample thicknesses and widths were measured at the specimen center with a Tacklife electronic digital sliding caliper (Levittown, NY, USA). The testing speed was set at 1 mm/min, with a 40 mm grip separation. Bending properties were characterized by testing the 16 specimens cut from the materials obtained after molding of each material. The evaluated properties were flexural modulus and flexural strength at breaking point, determined with the following formulas:

$$\text{Flexural modulus} = \frac{L^3}{4*w*t^3} * \frac{F_2 - F_1}{d_2 - d_1} \quad (2)$$

$$\text{Flexural strength} = F_{breaking} * \frac{3*L}{2*w*t^2} \quad (3)$$

where L is the length between the two supports, w is the sample width, t is the sample thickness, F_1 and F_2 are the forces measured for d_1 and d_2 deformations at 10 % and 40 % of $F_{breaking}$, respectively, and $F_{breaking}$ is the force measured at breaking point.

Water resistance was tested by immersing 45 mm long by 10 mm wide specimens in water at 25 °C to determine the water absorption (WA) and thickness swelling (TS) in triplicate according to the ISO 16983:2003 standard (ISO 16983:2003 Wood-Based Panels – Determination of Swelling in Thickness after Immersion in Water, 2003). Before soaking, samples were oven-dried at 105 °C until constant weight to ensure uniform initial conditions. The initial thickness and weight were then measured. The samples were subsequently submerged in distilled water at 25 °C for 24 h. The sample weights and thicknesses were measured hourly for the first 8 h and again after 24 h. The thickness of each sample was measured at three points: at the center and both ends. WA and TS were calculated per sample at 24 h using the following formulas:

$$WA = \frac{w_{24h} - w_0}{w_0} * 100 \quad (4)$$

$$TS = \frac{t_{24h} - t_0}{t_0} * 100 \quad (5)$$

where w_0 and w_{24h} are the sample weight initially and after 24 h of water immersion, and t_0 and t_{24h} are the sample thickness initially and after 24 h of water immersion.

2.7. Statistical analysis

WA, TS and density determinations were conducted in triplicate. For the mechanical properties, 16 samples were tested per extrusion condition. Means were statistically compared with a one-way analysis of variance (ANOVA) with $\alpha = 0.05$. A Student's *t* test was performed on the flexural strength and flexural modulus means, and values with no significant difference are presented with the same letter (a-d).

3. Results and discussion

3.1. Raw bagasse composition

The chemical composition of the SCB used in this study is presented in Table 2. With its main components being 40 % cellulose, 24 % lignin, 23 % hemicellulose and 5 % ash, its composition was in line with those reported in other previous studies, i.e. 36–45 % cellulose, 21–27 % lignin, 22–28 % hemicellulose and 3–9 % ash (de Rocha et al., 2015; Oriez et al., 2019; Yu et al., 2013).

3.2. SCB pretreatment by twin-screw extrusion

The overall SCB pretreatment results are presented in Table 3. For the three screw profiles, the experimental L/S ratios were close to those targeted, but the full L/S ratio range (0.4 – 2.0) was not achieved. Using profile 1, the high amperage (60 A) at 0.7 L/S ratio prevented us from studying lower L/S ratios due to the equipment safety limits. At low L/S ratios with this profile, the higher shear force during SCB processing increased the extruder motor power consumption, reaching the operational limits of the equipment. With profile 3, high L/S ratios could not be achieved due to substantial extruder clogging with water at L/S ratios > 1.25. This clogging was due to the limited passage created by the reverse screw elements used in this profile, causing water accumulation in the extruder up to the feeding module (module 1), thereby blocking the SCB inlet for these tests.

Table 2
Chemical composition of raw SCB (% DM).

Composition	SCB
Dry matter (%)	91.5 ± 0.1
Ash (%)	5.1 ± 0.2
AIL (%)	19.3 ± 0.2
ASL (%)	4.8 ± 0.1
Total Lignin (%)	**24.1 ± 0.3**
Cellulose (%)	**40.2 ± 0.3**
Xylan (%)	20.6 ± 0.1
Arabinan (%)	2.1 ± 0.1
Hemicellulose (%)	**22.7 ± 0.1**
Acetyl (%)	3.9 ± 0.1
Extractable H_2O + EtOH (%)	3.8 ± 0.7
Total (%)	100

With profile 1, the extrudate moisture content increased with the L/S ratio before reaching a plateau, i.e. a trend that was also observed with profiles 2 and 3. Extrudates were drier at lower L/S ratios due to a lower initial water input and higher evaporation rates, likely associated with greater self-heating in the vicinity of the CF2C reverse screw elements in module 7.

The amperage values were higher at lower L/S ratios for profiles 1 and 2, while remaining constant for profile 3 regardless of the L/S ratios, due to the higher shear forces exerted with profile 3. The reduction in current supplied to the extruder motor at higher L/S ratios could be attributed to the decreased shear forces during SCB processing, resulting from the increased water inlet flow rate and leading to a lower viscosity of the mixture within the extruder. These observations are consistent with the results of a previous study on SCB pretreatment by twin-screw extrusion with a configuration including a filtration module, where the measured amperage was higher for low L/S ratios (Cavailles et al., 2024a). In addition, for the same L/S ratio, the amperage increased with the severity of the screw profile. Previous studies have shown that electrical power and specific mechanical energy (SME) increased with more restrictive screw profile configurations (Altan et al., 2009; Gogoi et al., 1996). Decreasing the reverse screw element pitch (CF2C) and increasing its length resulted in higher amperage due to increased shear forces applied to the material in module 7. However, decreasing the reverse screw element pitch appeared to have a lesser effect than increasing its length when comparing profiles 2 and 3. A possible explanation for this is that increasing the length of the reverse screw element extended the exposure time of the material to shear forces, leading to better mixing and more uniform material processing, whereas reducing the pitch primarily slowed the material flow without significantly enhancing the overall shear or mixing efficiency.

Regarding water evaporation at the extruder outlet (Fig. 2), the proportion of water evaporated followed a bell curve according to changes in the L/S ratio. At lower L/S ratios, as the L/S ratio increased, there was an initial decrease in the amount and proportion of water evaporated, followed by an increase at higher L/S ratios. Water evaporation was higher with lower amounts of water in the extruder (low L/S ratios), due to an increased mixture viscosity and to the mechanical friction exerted in the vicinity of the reverse screw elements, thereby contributing to the self-heating of the material in module 7. Similar trends have been reported for rice straw (Theng et al., 2017) and SCB

Table 3
Production of SCB extrudates in the Clextral BC45 twin-screw extruder.

Trials	Profile	L/S	$Q_{SCB\ experimental}$ (kg $_{dry}$/h)	$Q_{L\ experimental}$ (kg/h)	Q_L/Q_S experimental	I (A)	Q_{EXT} (kg/h)	MC_{EXT} (%)	$Q_{EXT\ water}$ (kg/h)	E_w (kg/h)
1	1	0.70	5.9	3.9	**0.66**	60	7.2	17.6	1.3	2.6
2		0.85	5.2	4.3	**0.84**	40	8.6	40.3	3.5	0.8
3		1.00	5.0	5.0	**1.00**	36	8.4	40.2	3.4	1.6
4		1.25	4.9	6.2	**1.26**	40	8.3	40.1	3.3	2.9
5		1.50	4.3	7.2	**1.67**	36	7.0	38.2	2.7	4.5
6		2.00	5.3	10.1	**1.92**	40	8.6	38.6	3.3	6.8
7	2	0.40	5.5	2.2	**0.40**	65	6.2	11.2	0.7	1.5
8		0.55	8.1	4.0	**0.50**	41	10.6	24.0	2.5	1.5
9		0.70	6.0	3.9	**0.65**	41	9.6	37.6	3.6	0.3
10		0.85	7.1	5.1	**0.72**	45	12.3	42.6	5.2	0
11		1.00	5.8	5.3	**0.92**	48	10.6	45.0	4.8	0.6
12		1.25	5.2	6.3	**1.21**	45	9.0	41.9	3.8	2.6
13		1.50	5.0	7.5	**1.50**	36	8.8	43.1	3.8	3.7
14		2.00	5.5	10.2	**1.86**	36	9.3	41.4	3.9	6.3
15	3	0.40	6.3	2.7	**0.40**	53	7.2	12.2	0.9	1.8
16		0.70	7.0	4.4	**0.62**	53	10.1	30.7	3.1	1.2
17		1.00	6.2	5.2	**0.84**	54	9.1	31.3	2.8	2.4
18		1.25	4.4	5.5	**1.26**	54	5.7	22.6	1.3	4.3

Where L/S is the theoretical liquid-to-solid ratio, $Q_{SCB\ experimental}$ and $Q_{L\ experimental}$ are the experimental mass flow rates of SCB and water, QL/QS is the experimental liquid/solid ratio Q_{EXT} is the extrudate mass flow rate, MC_{EXT} is the moisture content of the extrudate, E_w is the evaporated water mass flow rate, and I is the amperage of the current drawn by the motor.

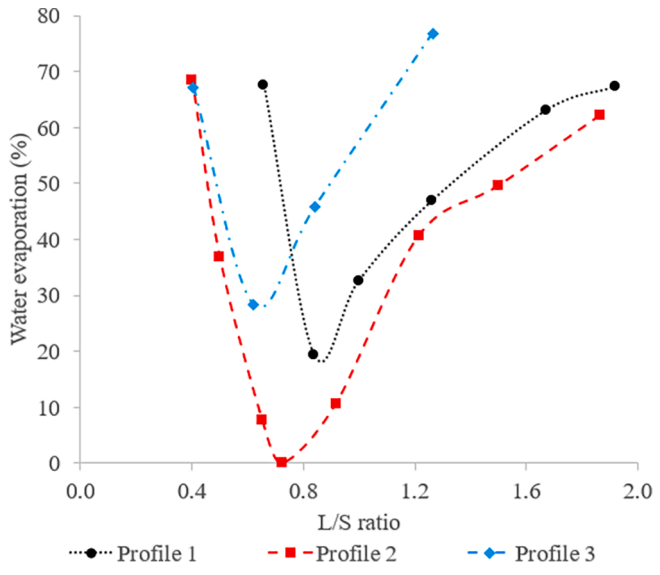

Fig. 2. Impact of the L/S ratio and screw profile on water evaporation during twin-screw extrusion.

(Cavailles et al., 2024a), with higher proportions of evaporated water noted at low L/S ratios. In the figure below, the second area of L/S ratios began at a ratio of 0.84 for profile 1, 0.72 for profile 2 and 0.62 for profile 3. In this second area, as the L/S ratio increased, the thermal conductivity and heat transfer in the mixture were improved with the addition of more water, hence amplifying the thermomechanical phenomena with the increase in the evaporated water quantity and proportion. It could also have been due to the rise in the free to bound water ratio. The proportion of free water increased with the L/S ratio, thus facilitating the evaporation of a higher proportion of water.

3.3. Physicochemical characterization of untreated SCB and extrudates

Binocular microscope observations on untreated SCB and extrudates are shown in Fig. 3, while the SEM images are presented in Fig. 4. Assessment of the twin-screw extrusion pretreatment effects on fibers revealed substantial morphological alteration. The optical and SEM images both indicated that untreated SCB consisted mostly of long (2–8 cm), intact fibers and a few spherical particles from the bagasse pith, with no individualized fibers. In contrast, clear fiber deconstruction was noted for all extrudates due to the extrusion process, leading to SCB defibration with finer, more individualized fibers and aggregates formed by fiber intermingling (Cavailles et al., 2024a).

A comparison of the optical and SEM images of extrudates obtained with the three screw profiles at a 1.25 L/S ratio (Figs. 3 and 4) showed that increasing the screw profile severity led to greater SCB defibration, with more individual fibers and a reduction in fiber and particle size.

Further comparisons of optical and SEM images of extrudates obtained with different L/S ratios per profile (Figs. 3 and 4) revealed distinct differences. For profile 1 at L/S ratios of 0.7 and 1.25, initial defibration was clearly visible for both ratios, showing the beginning of fiber breakage and individualization in some areas. For profile 2, the fibers were not individualized at a 0.4 L/S ratio, whereas individual fibers could be seen separating from the fiber slices at a 1.25 L/S ratio. For profile 3, the extrudate obtained at a 1.25 L/S ratio exhibited long individual fibers, whereas short fibers were obtained at a 0.4 L/S ratio. These observations suggest that a low 0.4 L/S ratio led to a grinding action, hence reducing the fiber and particle size, with relatively few individual fibers present, while a higher 1.25 L/S ratio promoted defibration with substantial fiber individualization. Moreover, reducing the L/S ratio resulted in more aggregates due to the higher mechanical action exerted on SCB, along with a decreased extrudate moisture content.

Aspect ratio measurements obtained on the binocular microscope images (Fig. 5) showed that, for all profiles, increasing the L/S ratio led to an increase in the fiber aspect ratios. A low L/S ratio resulted in a reduction in fiber size due to fiber cutting, as shown by the particle size distribution (Fig. 6), resulting in short fibers with lower aspect ratios, while a higher L/S ratio preserved the fiber length. At the same, the screw profile effect was clearcut at a 1.25 L/S ratio, with the aspect ratio decreasing as the screw profile shearing rate increased. A more shearing screw profile exerted greater constraints, in turn reducing the fiber size, as confirmed by the particle size distribution (Fig. 6) and thus the aspect ratio.

The particle size distribution results (Fig. 6) indicated that in the extrudates there was a tendency for fibers and particles to form aggregates $>$ 4 mm when dried, compared to untreated SCB. Twin-screw extrusion pretreatment resulted in a reduction in particle size, with a substantial increase in the proportion of fine particles ($<$0.2 mm). This phenomenon has been previously demonstrated with corn cobs (Zheng

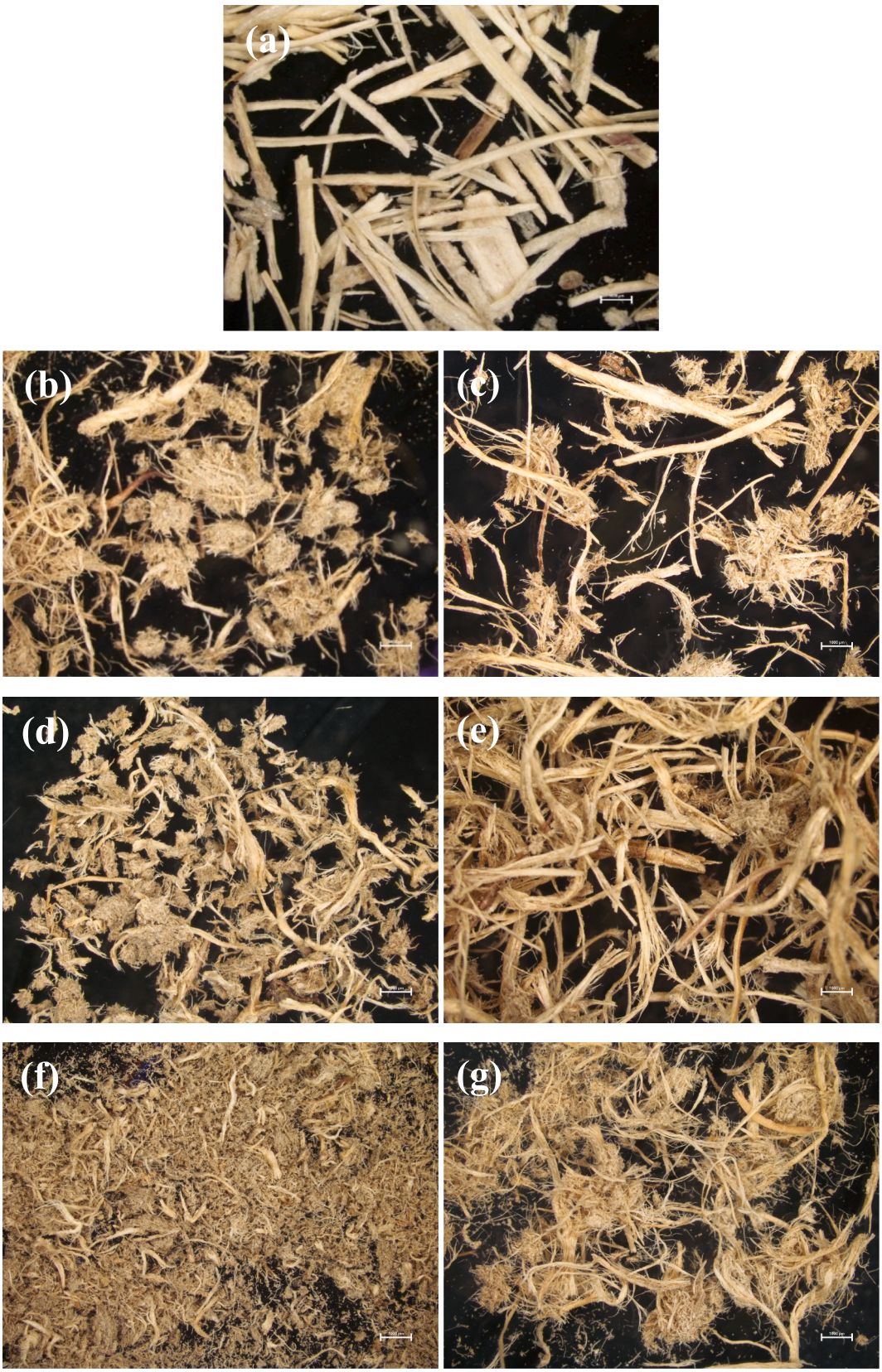

Fig. 3. Binocular microscope view of ground SCB before twin-screw extrusion pretreatment (a), and extrudates obtained with profile 1 at L/S ratios of 0.7 (b) and 1.25 (c), profile 2 at L/S ratios of 0.4 (d) and 1.25 (e), and profile 3 at L/S ratios of 0.4 (f) and 1.25 (g) (scale 1000 μm).

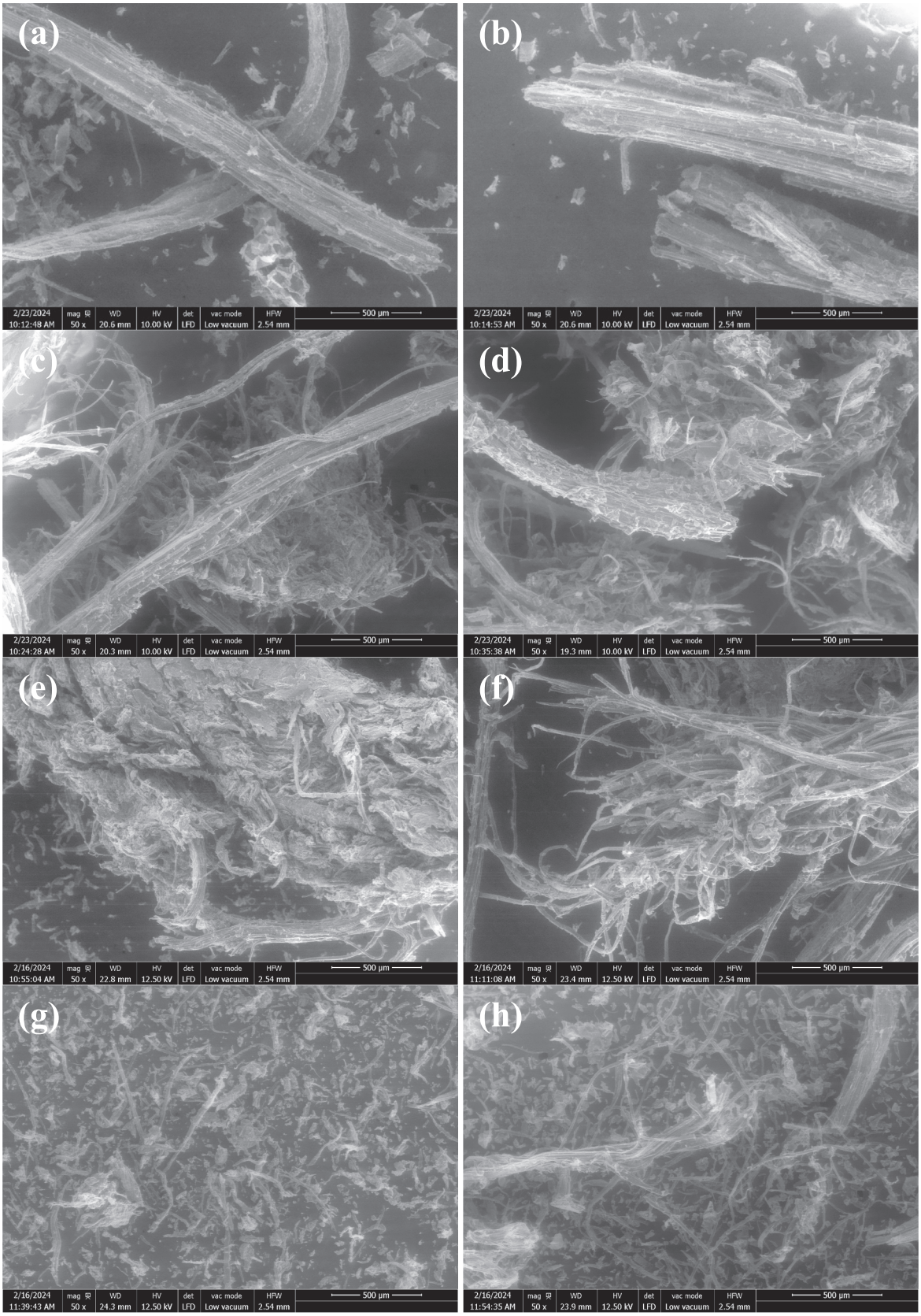

Fig. 4. SEM images at ×50 magnification of ground SCB prior twin-screw extrusion pretreatment (a-b), and extrudates obtained with profile 1 at L/S ratios of 0.7 (c) and 1.25 (d), profile 2 at L/S ratios of 0.4 (e) and 1.25 (f), and profile 3 at L/S ratios of 0.4 (g) and 1.25 (h).

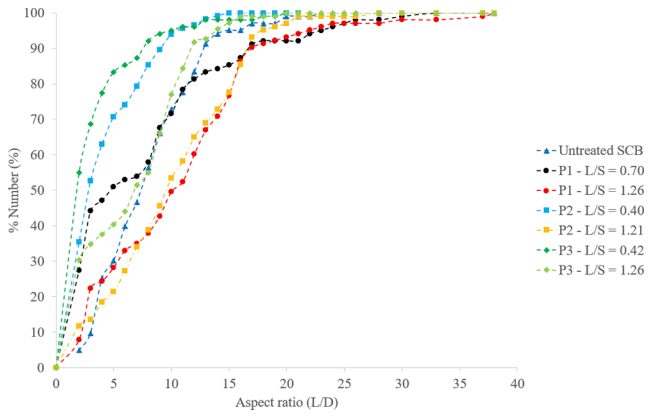

Fig. 5. Cumulative distribution of the aspect ratio for untreated SCB and extrudates obtained with different screw profiles and L/S ratios.

et al., 2015) and SCB (Cavailles et al., 2024a). The particle size reduction was due to shear friction between particles during the extrusion process.

For the three screw profiles, increasing the L/S ratio initially led to a decrease in the proportion of fine particles, reaching a minimum value before increasing again at higher L/S ratios. Overall, decreasing the L/S ratio resulted in a greater particle size reduction due to the lower water input and higher shearing forces exerted on the biomass fibers. Similar results have been obtained with hardwood (Senturk-Ozer et al., 2011) and rape straw (Um et al., 2013) at low L/S ratios. L/S ratios leading to the lowest proportion of fine particles were 1.26, 0.72 and 0.62 for screw profiles 1, 2 and 3, respectively, and this ratio decreased with increasing profile shear. A similar trend was observed with regard to water evaporation, with these same L/S ratios corresponding to minimal water evaporation. An increase in the proportion of fine particles was noted with more water evaporation, possibly because a greater quantity of water could reduce the viscosity of the mixture and the mechanical action exerted on the material, thus limiting particle size reduction in the extrudates. Another hypothesis is that the presence of more water might play a role in particle aggregation, allowing finer particles to aggregate with the fibers during extrudate drying.

A comparison of the effects of the three screw profiles on the particle size distribution at L/S ratios of around 0.65, 0.90 and 1.25 revealed that the proportion of 2 to 4 mm aggregates decreased with a more shearing screw profile, while the proportion of fine particles < 0.2 mm increased (Fig. 6d for 1.21–1.26 L/S ratios). Overall, screw profile 1 produced extrudates with the highest proportion of fibers or aggregates > 1 mm, screw profile 2 resulted in extrudates with the highest proportion of fibers in the 0.2–0.8 mm size range, and screw profile 3 led to extrudates containing the highest proportion of fine particles (< 0.2 mm). Pretreatment with a more restrictive screw profile resulted in an overall particle size reduction in the extrudate, linked to increased shear forces and friction between the biomass and the barrel, as well as reduced particle aggregation, which was in line with the binocular microscope and SEM image observations.

The bulk and tapped densities of the untreated SCB and extrudates are shown in Fig. 7. The extrudate bulk and tapped densities ranged from 34 to 147 kg/m^3, and from 50 to 212 kg/m^3, respectively. The extrudate densities were generally lower than those of untreated SCB, except for extrudates obtained with a 0.4 L/S ratio. Twin-screw extrusion pretreatment led to a reduction in the fiber density characteristics, which was associated with fiber deconstruction during thermo-mechanical pretreatment, resulting in the expansion and increased "fluffy" structure of SCB fibers. This trend was consistent with previous observations regarding SCB (Cavailles et al., 2024a), rice (Theng et al., 2019) and coriander (Uitterhaegen et al., 2017) straw fibers. The three screw profiles produced extrudates with similar bulk and tapped densities, indicating that the screw profile configuration had little impact on the extrudate density, in line with previous studies on maize grits (Ilo et al., 1996), barley grits and flour (Altan et al., 2009).

However, the L/S ratio had a substantial impact on the extrudate density. For all three profiles, the bulk and tapped densities were similar for L/S ratios between 0.5 and 2.0 due to the expanded morphological structure of the extrudates. As the L/S ratio decreased to 0.4, the bulk and tapped densities sharply increased to approximately 140 kg/m^3 and 210 kg/m^3, respectively, due to the increased pretreatment severity. At a 0.4 L/S ratio, the only water present originated from the SCB inherent

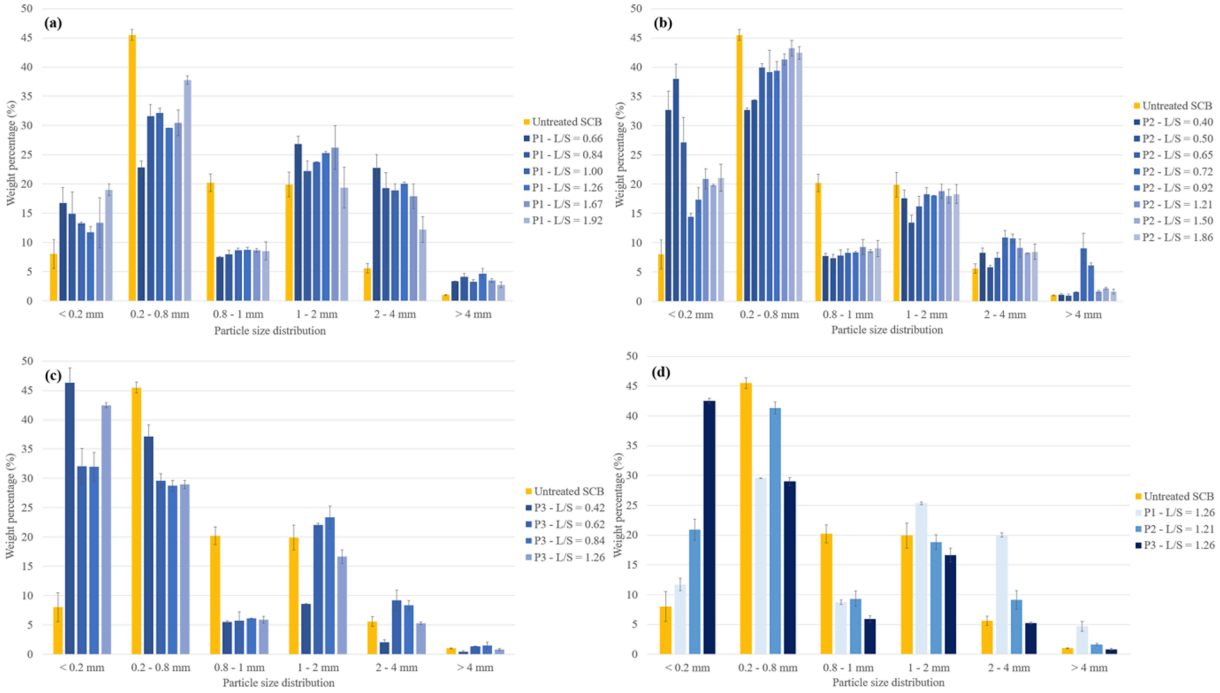

Fig. 6. Particle size distribution of untreated SCB and extrudates obtained with screw profiles 1 (a), 2 (b) and 3 (c) at different L/S ratios and with a L/S ratio of around 1.25 for the three screw profiles (d) (error bars represent standard deviations).

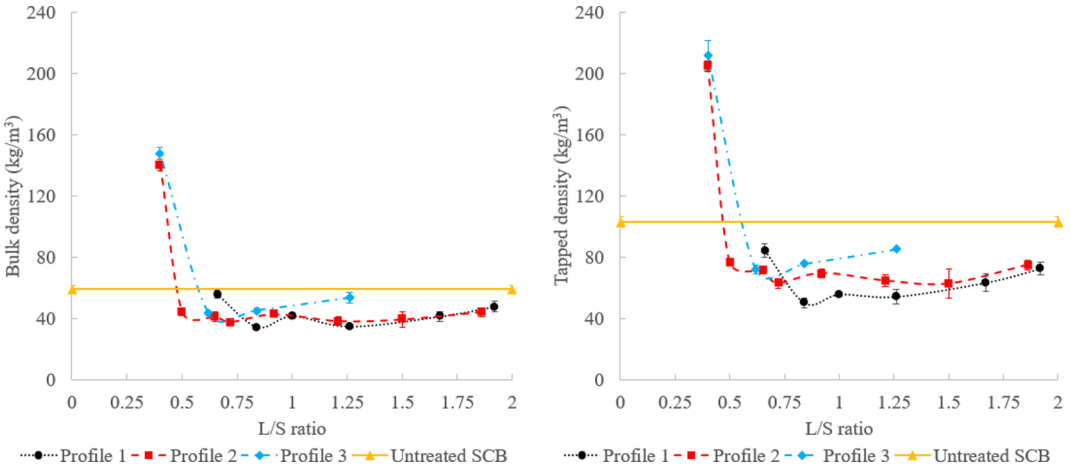

Fig. 7. Bulk and tapped densities of untreated SCB and extrudates obtained with different screw profiles and L/S ratios (error bars represent standard deviations).

moisture content. Under these conditions, the mixture in the extruder exhibited higher viscosity and was subject to stronger shear forces during the extrusion process, leading to fiber breakage (Senturk-Ozer et al., 2011; Uitterhaegen et al., 2017). This was shown by the increase in extruder amperage. The higher mechanical shearing and self-heating of the material at low L/S ratios resulted in more intense fiber cutting, with a reduction in particle size, as shown in the particle size distribution (Fig. 6), thereby promoting a higher extrudate density since the latter had fewer pores as they had been filled by the shorter fibers and finer particles. Under these extrusion conditions, the applied pretreatment was more akin to simple grinding than thermomechanical defibration. Similar results were reported with rice (Theng et al., 2019) and coriander (Uitterhaegen et al., 2017) straw extrudates obtained with a 0.4 L/S ratio.

Adsorption isotherms, determined on the basis of DVS measurements, are shown in Fig. 8. A comparison of untreated SCB with extrudates revealed that the pretreatment did not substantially modify the isotherms, which exhibited a type II shape (Fig. 8a). For the same L/S ratio (Fig. 8a), the adsorption isotherms of untreated SCB and extrudates obtained with different screw profiles were very similar, except for the extrudate from profile 1, which exhibited higher water adsorption. The SSA value of this extrudate was higher compared to those obtained with profiles 2 and 3. Destructuring SCB with different screw profiles modified the water adsorption behavior of the extrudates, and an increase in SSA and water adsorption constants led to the production of an extrudate that was more moisture sensitive as the applied shearing level decreased. Fig. 8b shows that increasing the L/S ratio during twin-screw extrusion pretreatment led to higher water adsorption at >50 % RH. At 95 % RH, the extrudate obtained with screw profile 2 and a 0.4 L/S ratio had 17.1 % water uptake, while the extrudate obtained with a L/S ratio of 1.86 had a much higher water uptake of 20.2 %. Moreover, the SSA calculated from the adsorption isotherms appeared to increase with the L/S ratio, whereas the water adsorption constants were similar. Destructuring SCB with a higher L/S ratio resulted in greater fiber individualization, as shown by the SEM images (Fig. 4), leading to an increased accessible surface area (Martins et al., 2018) and greater exposure of the hydrophilic functional groups such as hydroxyl groups on the cellulose and hemicellulose, facilitating water adsorption. Additionally, the porosity of the material may be enhanced, allowing more water to be retained within the internal structure of the fibers. This is

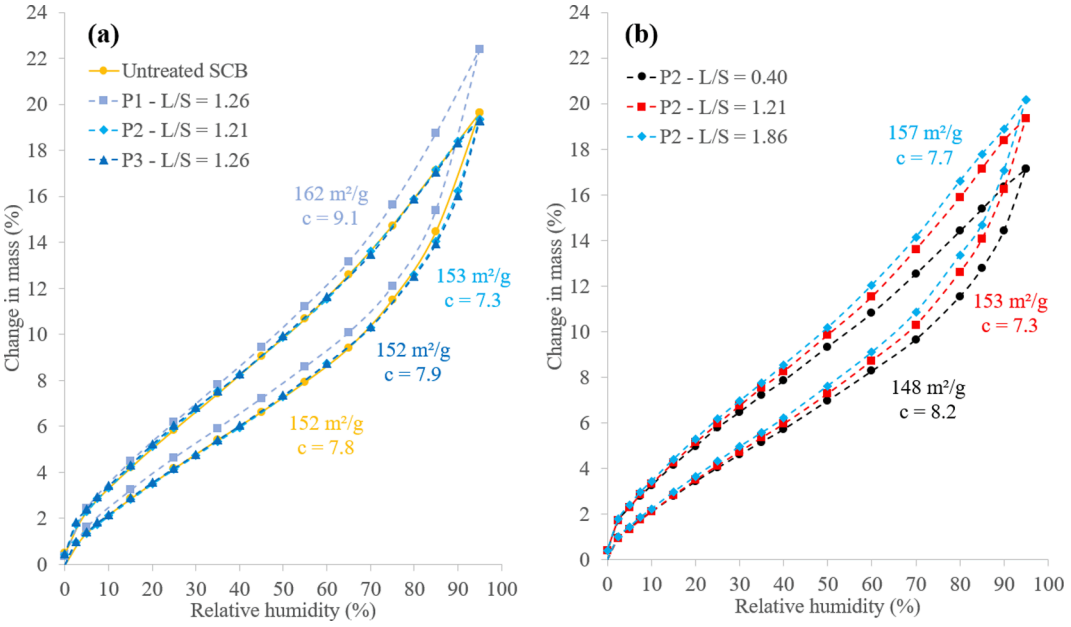

Fig. 8. Specific surface area, water adsorption constants and adsorption and desorption isotherms of extrudates obtained with different screw profiles compared to untreated SCB (a), and different L/S ratios (b).

supported by the observation of increased SSA with higher L/S ratios, which suggests the development of macropores that can act as water adsorption sites.

3.4. Thermocompression of binderless materials

The visual appearances of the materials obtained from untreated SCB and extrudates are presented in Fig. 9. There was a clear difference in fiber morphology when comparing the materials made from untreated SCB to extrudate-derived materials, as previously reported (Cavailles et al., 2024a). The material produced with untreated SCB exhibited longer surface fibers, whereas the materials produced with extrudates had a much more homogeneous appearance. All materials obtained by uniaxial thermocompression of extrudates had a smoother surface compared to the material derived from untreated SCB. The L/S ratio did not visually impact the appearance of the materials, but the screw profile tended to alter their appearance. Thermocompression of extrudates obtained with profile 3 resulted in materials with darker surfaces and a more homogeneous appearance, while materials obtained with extrudates from profiles 1 and 2 had lighter surfaces and heterogeneous edges. Extrudates obtained with profile 3 had higher proportions of fine particles (30–45 %) compared to those obtained with profile 1 (10–20 %) and 2 (15–35 %). During thermocompression, these fine particles probably filled the voids between fibers, hence resulting in a more compact material with a more homogeneous surface appearance.

3.4.1. Density and mechanical properties

The density and mechanical properties of materials obtained by thermocompression are presented in Table 4. All materials produced with extrudates had higher densities than those obtained from untreated SCB. This increase in density could be attributed to the higher proportion of fine particles in the extrudates due to fiber deconstruction, which acted as void filler, improving fiber contact and reducing the porosity in the final material (Cavailles et al., 2024b). However, the modification of the screw profile and L/S ratio had a minor impact on the material density. The flexural modulus and flexural strength of the materials were almost doubled with the addition of the twin-screw extrusion pretreatment to SCB. They ranged from 5.5 to 6.1 GPa, and from 39.0 to 55.5 MPa, respectively, for the materials obtained from the extrudates, whereas the material made with untreated SCB had a 3.3 GPa flexural modulus and 22.7 MPa flexural strength. Without pretreatment, due to the strong bonds between the cellulosic fibers and lignin within the structure, the lignin could not be mobilized to serve as a binder during thermocompression, resulting in reduced material cohesion and reduced mechanical resistance. Thermomechanical pretreatment could lead to the softening of lignin (Yoo et al., 2012) by reaching its glass transition temperature that start at 100 °C to 170 °C (Irvine, 1985) due to the increased temperature in the extruder (>100 °C) (Dittrich et al., 2021). Additionally, the water in the extruder could impact the lignin's glass transition, as an increase in the biomass's moisture content lowers the lignin's glass transition temperature (Bouajila et al., 2005). The thermomechanical defibration pretreatment likely disrupted the fiber structure, promoting the separation of cellulose, hemicelluloses and lignin, while homogenizing their size.

This improvement in mechanical properties using extruded fibers has been demonstrated in recent studies using SCB (Cavailles et al., 2024a), coriander straw (Uitterhaegen et al., 2017) and oleaginous flax straw shives (Evon et al., 2019). This suggested that defibration facilitated the separation of lignin and hemicelluloses from cellulose, in turn enhancing the role of lignin as a natural binder and promoting fiber assembly

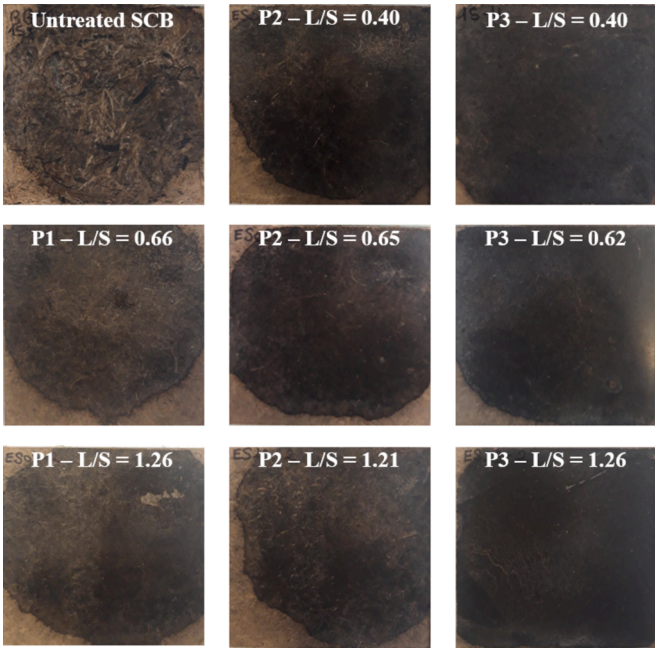

Fig. 9. Images of the materials generated by thermocompression of untreated SCB, and extruded SCB with different L/S ratios and screw profiles.

Table 4
Density, and mechanical properties of materials obtained with untreated SCB and extruded SCB using different screw profiles and L/S ratios.

N°	Sample	Density (kg/m^3)	Compaction ratio	Flexural strength (MPa)	Flexural modulus (GPa)
	Untreated SCB	1453 ± 6	24.1 ± 0.8	22.7 ± 7.5 ^{a}	3.3 ± 0.7 ^{a}
Screw profile 1					
1	L/S = 0.66	1488 ± 8	26.7 ± 1.2	44.8 ± 4.1$^{d, e}$	5.8 ± 0.7$^{b, c}$
2	L/S = 0.84	1480 ± 10	43.1 ± 1.1	51.1 ± 4.7$^{b, c}$	5.8 ± 0.8$^{b, c}$
3	L/S = 1.00	1474 ± 13	35.5 ± 1.6	50.2 ± 4.4$^{b, c}$	5.6 ± 0.7^{c}
4	L/S = 1.26	1480 ± 12	42.8 ± 1.6	48.6 ± 6.2$^{b, c, d}$	5.7 ± 0.7$^{b, c}$
5	L/S = 1.67	1478 ± 8	36.0 ± 2.8	51.0 ± 4.6$^{b, c}$	5.5 ± 0.5^{c}
6	L/S = 1.92	1496 ± 19	31.5 ± 2.2	51.5 ± 3.5^{b}	5.7 ± 0.5$^{b, c}$
Screw profile 2					
7	L/S = 0.40	1493 ± 10	10.6 ± 0.3	39.0 ± 1.7^{h}	6.0 ± 0.5$^{b, c}$
8	L/S = 0.50	1474 ± 15	33.4 ± 1.8	51.8 ± 6.1$^{b, g}$	5.9 ± 0.8$^{b, c}$
9	L/S = 0.65	1478 ± 34	36.0 ± 3.0	48.4 ± 4.8$^{c, f}$	5.8 ± 0.9$^{b, c}$
10	L/S = 0.72	1456 ± 53	38.7 ± 2.4	43.9 ± 3.9^{e}	5.9 ± 0.5$^{b, c}$
11	L/S = 0.92	1471 ± 9	34.5 ± 1.3	51.0 ± 7.0$^{b, c, g}$	6.1 ± 0.4^{b}
12	L/S = 1.21	1449 ± 17	38.0 ± 2.7	48.2 ± 6.7$^{b, c, d}$	6.0 ± 0.6$^{b, c}$
13	L/S = 1.50	1477 ± 9	34.9 ± 0.4	45.3 ± 7.7$^{d, e, f}$	5.9 ± 0.5$^{b, c}$
14	L/S = 1.86	1459 ± 13	33.1 ± 2.2	48.2 ± 8.0$^{b, c, d, e}$	5.5 ± 0.5^{c}
Screw profile 3					
15	L/S = 0.42	1498 ± 9	10.2 ± 0.3	45.9 ± 1.8$^{d, e, f}$	6.0 ± 0.5$^{b, c}$
16	L/S = 0.62	1477 ± 16	34.1 ± 1.2	52.4 ± 5.1$^{b, g}$	5.8 ± 0.6$^{b, c}$
17	L/S = 0.84	1471 ± 22	32.5 ± 1.1	54.7 ± 4.0^{g}	5.6 ± 0.4^{c}
18	L/S = 1.26	1468 ± 18	27.6 ± 1.8	55.5 ± 5.5^{g}	5.6 ± 0.4^{c}

Means in the flexural strength and flexural modulus columns with the same superscript letter (a-g) are not significantly different at $\alpha < 0.05$ according to the Student's test.

during thermocompression, thus contributing to material self-bonding. Moreover, defibration improved the fiber morphology, particularly the fiber aspect ratio (Fig. 5), thereby enhancing the mechanical properties of the resulting materials due to facilitated fiber entanglement.

The modification of the screw profile and L/S ratio did not have a significant impact on the flexural modulus. However, significant differences in flexural strength were observed depending on the twin-screw extrusion conditions. The lowest value was obtained with profile 2 and a 0.4 L/S ratio (39 MPa), while the highest value was obtained with profile 3 and a 1.26 L/S ratio (55.5 MPa). For screw profiles 1 and 2, the lower L/S ratio resulted in the lowest flexural strength, which was consistent with the results obtained with SCB pretreatment by twin-screw extrusion with filtration (Cavailles et al., 2024a). These results could be related to the extrudate density, as the density obtained with a 0.4 L/S ratio was at least twice that obtained with L/S ratios > 0.4 (Fig. 7). The fibers had a more expansive appearance, indicating greater porosity and a more accessible surface area. Higher L/S ratios produced extrudates with increased specific surface area of the particles, as confirmed by the SSA calculated from the adsorption isotherms (Fig. 8), and higher compaction ratios for the fibrous materials. This likely contributed to a better mechanical stress distribution in the material during the mechanical tests due to a higher number of areas of contact between the fibers and particles created during thermocompression, with more self-adhesion, thereby implying higher mechanical properties (Shen, 1986). Furthermore, for the same L/S ratio, the flexural strength increased with the shear severity of the screw profile. For an L/S ratio of around 0.65, the flexural strength was 44.8 MPa with screw profile 1, 48.4 MPa with screw profile 2, and 52.4 MPa with screw profile 3, with the latter being the most constraining. This trend was also observed at L/S ratios of around 0.90 and 1.25. Beaugrand and Berzin showed that the mechanical properties of lignocellulosic fiber-reinforced composites were higher when the screw profiles were more severe due to greater defibration of the initial bundles and the creation of more stress transfer interfaces (Beaugrand and Berzin, 2013). The binocular microscope and SEM images (Fig. 4) confirmed that defibration increased with the screw profile severity, which may explain the improvement in mechanical properties.

3.4.2. *Water resistance*

WA and TS after 24 h water immersion of the materials obtained by thermocompression are shown in Fig. 10. WA and TS ranged from 25 to 62 %, and from 25 to 67 %, respectively. Material made from untreated SCB showed much higher WA (95 %), and TS (84 %). This could be attributed to the lower density of the material derived from untreated SCB, i.e. lower density values indicate higher material porosity, allowing more water penetration into the material structure. Similarly, a reduction in WA and TS was reported for materials made with extruded SCB (Cavailles et al., 2024a) and oleaginous flax straw shives (Evon et al., 2019) compared to materials made from raw material. The effects of the screw profile were clearly visible: for the same L/S ratio, water resistance improved with the most shearing screw profile. Considering the DVS results, where the water uptake of the extrudate obtained with profile 1 was higher than that of the extrudates obtained with profiles 2 and 3, it was clear that an extrudate with a higher adsorption capacity produced a more moisture-sensitive material with higher WA and TS values. The adsorption isotherms were similar for materials obtained from extrudates produced with profiles 2 and 3, and the observed differences in WA and TS were therefore directly linked to the thermocompression shaping of the materials. Shaping a more defibrated extrudate with a higher proportion of fine particles, i.e. obtained by using a more restrictive screw profile, contributed to reducing the internal porosity of the materials, resulting in more interparticle bonding, and preventing water penetration.

Regarding the L/S ratios, the trends showed a reduction in WA and TS with decreasing L/S ratios, which was consistent with the DVS measurements (Fig. 8), where decreasing the L/S ratio for extrudate production led to a decrease in adsorbed water uptake. Application of the lowest 0.4 L/S ratio resulted in a material with the best water resistance, likely due to the lower specific surface area, higher fine particle proportion, and higher extrudate density. The water sensitivity of the materials was directly linked to their density. Extrudates with a 0.4 L/S ratio were more compact, with a denser bed of material before thermocompression, which produced thinner and denser materials, with a lower accessible surface area and fewer water absorption areas, hence preventing water penetration into the material structure. Similar results were obtained with coriander straw fiberboards (Uitterhaegen et al., 2017).

4. Conclusion

New bio-based materials were manufactured by thermocompression exclusively from SCB extrudates produced through twin-screw extrusion as a thermomechanical pretreatment. This process facilitated SCB deconstruction, resulting in fiber defibration and modification of the fiber morphological structure, leading to lower densities. It also led to substantial particle size reduction and the formation of aggregates on the extrudates, contributing to greater material densification compared to untreated SCB. A comparison of the mechanical properties and water resistance of the materials clearly demonstrated the superior properties of those derived from extrudates. The choice of screw profile and L/S ratio for extrudate production impacted the mechanical properties and water resistance of the final materials and best conditions for this

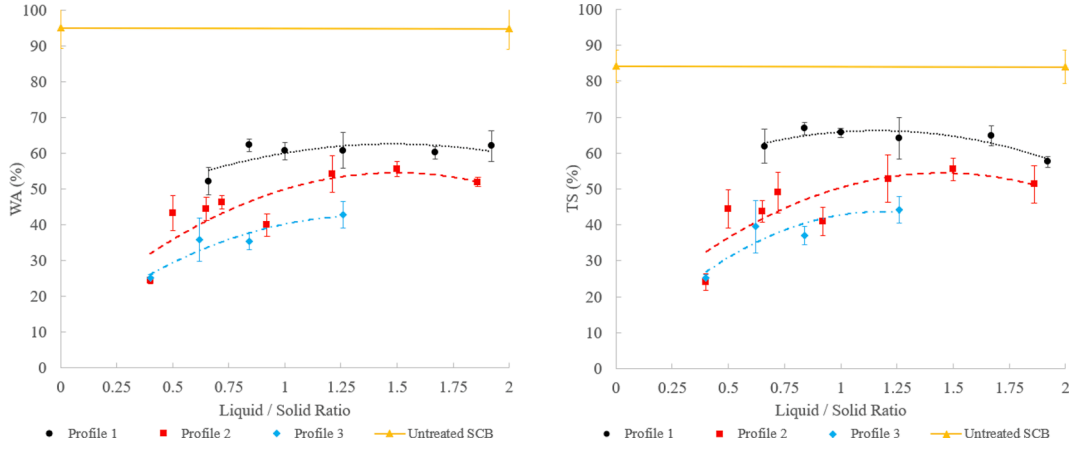

Fig. 10. WA and TS of thermocompressed materials obtained from untreated SCB and extrudates with different screw profiles and L/S ratios (error bars represent standard deviations).

pretreatment depend on the desired material properties. The best flexural properties were observed in materials made from extrudates produced at a 1.25 L/S ratio with screw profile 3, i.e. the most shearing one, while the best water resistance was noted in materials made from extrudates obtained at a 0.4 L/S ratio with screw profiles 2 and 3. In all cases, selecting a more shearing screw profile results in a material with better mechanical properties and water resistance. For the L/S ratio, a compromise must be found between achieving high mechanical properties at a high L/S ratio and higher water resistance at a low L/S ratio.

CRediT authorship contribution statement

Julie Cavailles: Writing – original draft, Visualization, Methodology, Investigation, Formal analysis, Conceptualization. **Guadalupe Vaca-Medina:** Writing – review & editing, Validation, Supervision, Methodology, Investigation, Conceptualization. **Jenny Wu-Tiu-Yen:** Writing – review & editing, Validation, Supervision, Resources, Project administration, Funding acquisition. **Laurent Labonne:** Writing – review & editing, Investigation. **Philippe Evon:** Writing – review & editing, Investigation. **Jérôme Peydecastaing:** Writing – review & editing, Validation, Supervision, Resources, Project administration, Methodology, Funding acquisition, Conceptualization. **Pierre-Yves Pontalier:** Writing – review & editing, Validation, Supervision, Resources, Project administration, Methodology, Funding acquisition, Conceptualization.

Declaration of competing interest

The authors declare that they have no known competing financial interests or personal relationships that could have appeared to influence the work reported in this paper.

Acknowledgements

This work was supported by the French National Association for Research and Technology (ANRT) under grant number 2021/0625 and supported by a French government grant managed by the French National Agency for Research (ANR) as part of the Investments for the Future program under the reference ANR-18-EURE-0021.

Data availability

Data will be made available on request.

References

Alokika, A., Kumar, A., Kumar, V., Singh, B., 2021. Cellulosic and hemicellulosic fractions of sugarcane bagasse: potential, challenges and future perspective. Int. J. Biol. Macromol. 169, 564–582. https://doi.org/10.1016/j.ijbiomac.2020.12.175.

Altan, A., McCarthy, K.L., Maskan, M., 2009. Effect of screw configuration and raw material on some properties of barley extrudates. J. Food Eng. 92, 377–382. https://doi.org/10.1016/j.jfoodeng.2008.12.010.

Alvarez, V., Iannoni, A., Kenny, J.M., Vázquez, A., 2005. Influence of twin-screw processing conditions on the mechanical properties of biocomposites. J. Compos. Mater. 39, 2023–2038. https://doi.org/10.1177/0021998305052025.

Anuar, H., Zuraida, A., Kovacs, J.G., Tabi, T., 2012. Improvement of mechanical properties of injection-molded polylactic acid-kenaf fiber biocomposite. J. Thermoplast. Compos. Mater. 25, 153–164. https://doi.org/10.1177/0892705711408984.

Anwar, Z., Gulfraz, M., Irshad, M., 2014. Agro-industrial lignocellulosic biomass a key to unlock the future bio-energy: a brief review. J. Radiat. Res. Appl. Sci. 7, 163–173. https://doi.org/10.1016/j.jrras.2014.02.003.

Arshad, M., Ahmed, S., 2016. Cogeneration through bagasse: a renewable strategy to meet the future energy needs. Renew. Sustain. Energy Rev. 54, 732–737. https://doi.org/10.1016/j.rser.2015.10.145.

Beaugrand, J., Berzin, F., 2013. Lignocellulosic fiber reinforced composites: influence of compounding conditions on defibrization and mechanical properties. J. Appl. Polym. Sci. 128, 1227–1238. https://doi.org/10.1002/app.38468.

Bouajila, J., Limare, A., Joly, C., Dole, P., 2005. Lignin plasticization to improve binderless fiberboard mechanical properties. Polym. Eng. Sci. 45, 809–816. https://doi.org/10.1002/pen.20342.

Brunauer, S., Emmett, P.H., Teller, E., 1938. Adsorption of gases in multimolecular layers. J. Am. Chem. Soc. 60, 309–319. https://doi.org/10.1021/ja01269a023.

Cavailles, J., Vaca-Medina, G., Wu-Tiu-Yen, J., Labonne, L., Evon, P., Peydecastaing, J., Pontalier, P.-Y., 2024a. Aqueous Pretreatment of Lignocellulosic Biomass for Binderless Material Production: Influence of Twin-Screw Extrusion Configuration and Liquid-to-Solid Ratio. Molecules 29, 3020. https://doi.org/10.3390/molecules29133020.

Cavailles, J., Vaca-Medina, G., Wu-Tiu-Yen, J., Peydecastaing, J., Pontalier, P.-Y., 2024b. Influence of Thermocompression Conditions on the Properties and Chemical Composition of Bio-Based Materials Derived from Lignocellulosic Biomass. Materials 17, 1713. https://doi.org/10.3390/ma17081713.

Chen, W.-H., Xu, Y.-Y., Hwang, W.-S., Wang, J.-B., 2011. Pretreatment of rice straw using an extrusion/extraction process at bench-scale for producing cellulosic ethanol. Bioresour. Technol. 102, 10451–10458. https://doi.org/10.1016/j.biortech.2011.08.118.

da Silva, A.S., Teixeira, R.S.S., Endo, T., Bon, E.P.S., Lee, S.-H., 2013. Continuous pretreatment of sugarcane bagasse at high loading in an ionic liquid using a twin-screw extruder. Green Chem. 15, 1991. https://doi.org/10.1039/c3gc40352a.

de Rocha, G.J., Nascimento, V.M., Gonçalves, A.R., Silva, V.F.N., Martín, C., 2015. Influence of mixed sugarcane bagasse samples evaluated by elemental and physical–chemical composition. Ind. Crops Prod. 64, 52–58. https://doi.org/10.1016/j.indcrop.2014.11.003.

Dittrich, C., Pecenka, R., Løes, A.-K., Cáceres, R., Conroy, J., Rayns, F., Schmutz, U., Kir, A., Kruggel-Emden, H., 2021. Extrusion of different plants into fibre for peat replacement in growing media: adjustment of parameters to achieve satisfactory physical fibre-properties. Agronomy 11, 1185. https://doi.org/10.3390/agronomy11061185.

Duque, A., Manzanares, P., González, A., Ballesteros, M., 2018. Study of the application of alkaline extrusion to the pretreatment of eucalyptus biomass as first step in a bioethanol production process. Energies 11, 2961. https://doi.org/10.3390/en11112961.

Evon, Ph., Amalia Kartika, I., Cerny, M., Rigal, L., 2013. Extraction of oil from jatropha seeds using a twin-screw extruder: Feasibility study. Ind. Crops Prod. 47, 33–42. https://doi.org/10.1016/j.indcrop.2013.02.034.

Evon, P., Barthod-Malat, B., Grégoire, M., Vaca-Medina, G., Labonne, L., Ballas, S., Véronèse, T., Ouagne, P., 2019. Production of fiberboards from shives collected after continuous fiber mechanical extraction from oleaginous flax. J. Nat. Fibers 16, 453–469. https://doi.org/10.1080/15440478.2017.1423264.

Evon, P., Labonne, L., Khan, S.U., Ouagne, P., Pontalier, P.-Y., Rouilly, A., 2021. Twin-Screw Extrusion Process to Produce Renewable Fiberboards. J. Vis. Exp. 62072. https://doi.org/10.3791/62072.

Evon, P., Vandenbossche, V., Candy, L., Pontalier, P.-Y., Rouilly, A., 2018, 1st Edition. ACS Symposium Series. American Chemical Society, Washington, DC, pp. 25–44. https://doi.org/10.1021/bk-2018-1304.ch002.

Evon, Ph., Vandenbossche, V., Pontalier, P.Y., Rigal, L., 2009. Aqueous extraction of residual oil from sunflower press cake using a twin-screw extruder: Feasibility study. Ind. Crops Prod. 29, 455–465. https://doi.org/10.1016/j.indcrop.2008.09.001.

Evon, P., Vandenbossche, V., Pontalier, P.-Y., Rigal, L., 2014. New thermal insulation fiberboards from cake generated during biorefinery of sunflower whole plant in a twin-screw extruder. Ind. Crops Prod. 52, 354–362. https://doi.org/10.1016/j.indcrop.2013.10.049.

FAO, 2021. FAOSTAT. Food Agric. Organ. U. N. Stat. Div.

Gamon, G., Evon, Ph., Rigal, L., 2013. Twin-screw extrusion impact on natural fibre morphology and material properties in poly(lactic acid) based biocomposites. Ind. Crops Prod. 46, 173–185. https://doi.org/10.1016/j.indcrop.2013.01.026.

Gao, Y., Xia, H., Sulaeman, A.P., De Melo, E.M., Dugmore, T.I., Matharu, A.S., 2019. Defibrillated celluloses via dual twin-screw extrusion and microwave hydrothermal treatment of spent pea biomass. ACS Sustain. Chem. Eng. 7, 11861–11871. https://doi.org/10.1021/acssuschemeng.9b02440.

Gogoi, B.K., Oswalt, A.J., Choudhary, G.S., 1996. Reverse screw elements and feed composition effects during twin-screw extrusion of rice flour and fish muscle blends. J. Food Sci. 61, 590–595. https://doi.org/10.1111/j.1365-2621.1996.tb13165.x.

Harmsen, P., Huijgen, W., Bermudez, L., Bakker, R., 2010. Literature Review of Physical and Chemical Pretreatment Processes for Lignocellulosic Biomass. UR-Food Biobased Res, Wagening.

Ilo, S., Tomschik, U., Berghofer, E., Mundigler, N., 1996. The effect of extrusion operating conditions on the apparent viscosity and the properties of extrudates in twin-screw extrusion cooking of maize grits. LWT - Food Sci. Technol. 29, 593–598. https://doi.org/10.1006/fstl.1996.0092.

International Organization for Standardization. 2003. ISO 16978:2003 Wood-Based Panels - Determination of Modulus of Elasticity in Bending and of Bending Strength, 2003.

International Organization for Standardization. 2003. ISO 16983:2003 Wood-Based Panels - Determination of Swelling in Thickness after Immersion in Water, 2003.

Irvine, G.M., 1985. The significance of the glass transition of lignin in thermomechanical pulping. Wood Sci. Technol. 19, 139–149. https://doi.org/10.1007/BF00353074.

Kang, K.E., Han, M., Moon, S.-K., Kang, H.-W., Kim, Y., Cha, Y.-L., Choi, G.-W., 2013. Optimization of alkali-extrusion pretreatment with twin-screw for bioethanol production from Miscanthus. Fuel 109, 520–526. https://doi.org/10.1016/j.fuel.2013.03.026.

Karp, S.G., Woiciechowski, A.L., Soccol, V.T., Soccol, C.R., 2013. Pretreatment strategies for delignification of sugarcane bagasse: a review. Braz. Arch. Biol. Technol. 56, 679–689. https://doi.org/10.1590/S1516-89132013000400019.

Konan, D., Koffi, E., Ndao, A., Peterson, E.C., Rodrigue, D., Adjallé, K., 2022. An overview of extrusion as a pretreatment method of lignocellulosic biomass. Energies 15, 3002. https://doi.org/10.3390/en15093002.

Kuster Moro, M., Teixeira, S.S., Sant'Ana Da Silva, A., Duarte Fujimoto, M., Albuquerque Melo, P., Resende Secchi, A., Pinto Da Silva, E., Bon, 2017. Continuous pretreatment of sugarcane biomass using a twin-screw extruder. Ind. Crops Prod. 97, 509–517. https://doi.org/10.1016/j.indcrop.2016.12.051.

Lamsal, B., Yoo, J., Brijwani, K., Alavi, S., 2010. Extrusion as a thermo-mechanical pretreatment for lignocellulosic ethanol. Biomass Bioenergy 34, 1703–1710. https://doi.org/10.1016/j.biombioe.2010.06.009.

Mankar, A.R., Pandey, A., Modak, A., Pant, K.K., 2021. Pretreatment of lignocellulosic biomass: a review on recent advances. Bioresour. Technol. 334, 125235. https://doi.org/10.1016/j.biortech.2021.125235.

Martins, E.H., Vilela, A.P., Mendes, R.F., Mendes, L.M., Vasconcellos de Siqueira Brandão Vaz, L.E., Guimarães Junior, J.B., 2018. Soybean waste in particleboard production. Ciênc. E Agrotecnologia 42, 186–194. https://doi.org/10.1590/1413-70542018422015817.

Meghana, M., Shastri, Y., 2020. Sustainable valorization of sugar industry waste: Status, opportunities, and challenges. Bioresour. Technol. 303, 122929. https://doi.org/10.1016/j.biortech.2020.122929.

N'Diaye, S., Rigal, L., 2000. Factors influencing the alkaline extraction of poplar hemicelluloses in a twin-screw reactor: correlation with specific mechanical energy and residence time distribution of the liquid phase. Bioresour. Technol. https://doi.org/10.1016/S0960-8524(00)00032-8.

Nadhari, W.N.A.W., Karim, N.A., Boon, J.G., Salleh, K.M., Mustapha, A., Hashim, R., Sulaiman, O., Azni, M.E., 2020. Sugarcane (Saccharum officinarium L.) bagasse binderless particleboard: effect of hot pressing time study. Mater. Today Proc. 31, 313–317. https://doi.org/10.1016/j.matpr.2020.06.016.

Nonaka, S., Umemura, K., Kawai, S., 2013. Characterization of bagasse binderless particleboard manufactured in high-temperature range. J. Wood Sci. 59, 50–56. https://doi.org/10.1007/s10086-012-1302-6.

Oriez, V., Peydecastaing, J., Pontalier, P.-Y., 2019. Separation of sugarcane bagasse mild alkaline extract components by ultrafiltration – Membrane screening and effect of filtration parameters. Process Biochem 78, 91–99. https://doi.org/10.1016/j.procbio.2019.01.006.

Pérez-Rodríguez, N., García-Bernet, D., Domínguez, J.M., 2017. Extrusion and enzymatic hydrolysis as pretreatments on corn cob for biogas production. Renew. Energy 107, 597–603. https://doi.org/10.1016/j.renene.2017.02.030.

Ramaraj, B., 2007. Mechanical and thermal properties of polypropylene/sugarcane Bagasse composites. J. Appl. Polym. Sci. 103, 3827–3832. https://doi.org/10.1002/app.25333.

Rouilly, A., Jorda, J., Rigal, L., 2006. Thermo-mechanical processing of sugar beet pulp. I. Twin-screw extrusion process. Carbohydr. Polym. 66, 81–87. https://doi.org/10.1016/j.carbpol.2006.02.025.

Sasimowski, E., Majewski, Ł., Grochowicz, M., 2021. Efficiency of twin-screw extrusion of biodegradable poly (butylene succinate)-wheat bran blend. Materials 14, 424. https://doi.org/10.3390/ma14020424.

Satyanarayana, K.G., Flores-Sahagun, T.H.S., Bowman, P., 2018. Lignocellulosic materials of Brazil – their characterization and applications in polymer composites and art works. In: Kalia, S. (Ed.), Lignocellulosic Composite Materials, Springer Series on Polymer and Composite Materials. Springer International Publishing, Cham, pp. 1–96. https://doi.org/10.1007/978-3-319-68696-7_1.

Semple, K.E., Zhou, C., Rojas, O.J., Nkeuwa, W.N., Dai, C., 2022. Moulded pulp fibers for disposable food packaging: a state-of-the-art review. Food Packag. Shelf Life 33, 100908. https://doi.org/10.1016/j.fpsl.2022.100908.

Senturk-Ozer, S., Gevgilili, H., Kalyon, D.M., 2011. Biomass pretreatment strategies via control of rheological behavior of biomass suspensions and reactive twin screw extrusion processing. Bioresour. Technol. 102, 9068–9075. https://doi.org/10.1016/j.biortech.2011.07.018.

Shen, K.C., 1986. Process for Manufacturing Composite Products from Lignocellulosic Materials. 4,627,951.

Singh, S.P., Jawaid, M., Chandrasekar, M., Senthilkumar, K., Yadav, B., Saba, N., Siengchin, S., 2021. Sugarcane wastes into commercial products: processing methods, production optimization and challenges. J. Clean. Prod. 328, 129453. https://doi.org/10.1016/j.jclepro.2021.129453.

Sluiter, A., Hames, B., Ruiz, R., Scarlata, C., Sluiter, J., Templeton, D., Crocker, D., 2008. Determination of structural carbohydrates and lignin in biomass. Lab. Anal. Proced. LAP 1617, 1–16.

Sluiter, A., 2008. Determination of Total Solids in Biomass and Total Dissolved Solids in Liquid Process Samples: Laboratory Analytical Procedure (LAP). Tech. Rep.

Sriti, J., Msaada, K., Talou, T., Faye, M., Kartika, I.A., Marzouk, B., 2012. Extraction of coriander oil by twin-screw extruder: screw configuration and operating conditions effect. Ind. Crops Prod. 40, 355–360. https://doi.org/10.1016/j.indcrop.2012.03.034.

Sugahara, E.S., da Silva, S.A.M., Buzo, A.L.S.C., de Campos, C.I., Morales, E.A.M., Ferreira, B.S., dos Azamnuja, M., Lahr, F.A.R., Christoforo, A.L., 2019. High-density particleboard made from agro-industrial waste and different adhesives. BioResources 14, 5162–5170. https://doi.org/10.15376/biores.14.3.5162-5170.

Theng, D., Arbat, G., Delgado-Aguilar, M., Ngo, B., Labonne, L., Evon, P., Mutjé, P., 2017. Comparison between two different pretreatment technologies of rice straw fibers prior to fiberboard manufacturing: Twin-screw extrusion and digestion plus defibration. Ind. Crops Prod. 107, 184–197. https://doi.org/10.1016/j.indcrop.2017.05.049.

Theng, D., Arbat, G., Delgado-Aguilar, M., Ngo, B., Labonne, L., Mutjé, P., Evon, P., 2019. Production of fiberboard from rice straw thermomechanical extrudates by thermopressing: influence of fiber morphology, water and lignin content. Eur. J. Wood Wood Prod. 77, 15–32. https://doi.org/10.1007/s00107-018-1358-0.

Uitterhaegen, E., Parinet, J., Labonne, L., Mérian, T., Ballas, S., Véronèse, T., Merah, O., Talou, T., Stevens, C.V., Chabert, F., Evon, Ph., 2018. Performance, durability and recycling of thermoplastic biocomposites reinforced with coriander straw. Compos. Part Appl. Sci. Manuf. 113, 254–263. https://doi.org/10.1016/j.compositesa.2018.07.038.

Uitterhaegen, E., Evon, P., 2017. Twin-screw extrusion technology for vegetable oil extraction: A review. J. Food Eng. 212, 190–200. https://doi.org/10.1016/j.jfoodeng.2017.06.006.

Uitterhaegen, E., Labonne, L., Merah, O., Talou, T., Ballas, S., Véronèse, T., Evon, P., 2017. Impact of Thermomechanical Fiber Pre-Treatment Using Twin-Screw Extrusion on the Production and Properties of Renewable Binderless Coriander Fiberboards. Int. J. Mol. Sci. 18, 1539. https://doi.org/10.3390/ijms18071539.

Uitterhaegen, E., Nguyen, Q.H., Sampaio, K.A., Stevens, C.V., Merah, O., Talou, T., Rigal, L., Evon, Ph., 2015. Extraction of Coriander Oil Using Twin-Screw Extrusion: Feasibility Study and Potential Press Cake Applications. J. Am. Oil Chem. Soc. 92, 1219–1233. https://doi.org/10.1007/s11746-015-2678-4.

Um, B.-H., Choi, C.H., Oh, K.K., 2013. Chemicals effect on the enzymatic digestibility of rape straw over the thermo-mechanical pretreatment using a continuous twin screw-driven reactor (CTSR). Bioresour. Technol. 130, 38–44. https://doi.org/10.1016/j.biortech.2012.12.077.

Vandenbossche, V., Brault, J., Hernandez-Melendez, O., Evon, P., Barzana, E., Vilarem, G., Rigal, L., 2016. Suitability assessment of a continuous process combining thermo-mechano-chemical and bio-catalytic action in a single pilot-scale twin-screw extruder for six different biomass sources. Bioresour. Technol. 211, 146–153. https://doi.org/10.1016/j.biortech.2016.03.072.

Wang, L., Tong, Z., Ingram, L.O., Cheng, Q., Matthews, S., 2013. Green composites of poly (lactic acid) and sugarcane bagasse residues from bio-refinery processes. J. Polym. Environ. 21, 780–788. https://doi.org/10.1007/s10924-013-0601-3.

Widyorini, R., Xu, J., Umemura, K., Kawai, S., 2005. Manufacture and properties of binderless particleboard from bagasse I: effects of raw material type, storage methods, and manufacturing process. J. Wood Sci. 51, 648–654. https://doi.org/10.1007/s10086-005-0713-z.

Yoo, J., Alavi, S., Vadlani, P., Behnke, K.C., 2012. Soybean hulls pretreated using thermo-mechanical extrusion—hydrolysis efficiency, fermentation inhibitors, and ethanol yield. Appl. Biochem. Biotechnol. 166, 576–589. https://doi.org/10.1007/s12010-011-9449-y.

Yu, Q., Zhuang, X., Lv, S., He, M., Zhang, Y., Yuan, Z., Qi, W., Wang, Q., Wang, W., Tan, X., 2013. Liquid hot water pretreatment of sugarcane bagasse and its comparison with chemical pretreatment methods for the sugar recovery and structural changes. Bioresour. Technol. 129, 592–598. https://doi.org/10.1016/j.biortech.2012.11.099.

Zeitoun, R., 2010. Twin-screw extrusion for hemicellulose recovery: Influence on extract purity and purification performance. Bioresour. Technol. https://doi.org/10.1016/j.biortech.2010.07.022.

Zheng, J., 2016. Xylose removal from lignocellulosic biomass via a twin-screw extruder: the effects of screw configurations and operating conditions. Biomass Bioenergy. https://doi.org/10.1016/j.biombioe.2016.03.012.

Zheng, J., Choo, K., Rehmann, L., 2015. The effects of screw elements on enzymatic digestibility of corncobs after pretreatment in a twin-screw extruder. Biomass Bioenergy 74, 224–232. https://doi.org/10.1016/j.biombioe.2015.01.022.

Zheng, J., Rehmann, L., 2014. Extrusion pretreatment of lignocellulosic biomass: a review. Int. J. Mol. Sci. 15, 18967–18984. https://doi.org/10.3390/ijms151018967.